APPLIED RESEARCH

Elastic Modulus Adjustment Method of Double-Stator HTS Field Modulated Machine Based on Entire Machine Modal Analysis

YUBIN WANG[1], **CHUNTONG SONG**[1],
ZHIHENG ZHANG[2], **(Graduate Student Member, IEEE),**
AND WEI HUA[2], **(Senior Member, IEEE)**
[1]College of New Energy, China University of Petroleum (East China), Qingdao 266580, China
[2]School of Electrical Engineering, Southeast University, Nanjing 210096, China

Corresponding author: Yubin Wang (wangyubin@upc.edu.cn)

ABSTRACT The double stator high-temperature superconducting field modulated (DS-HTS-FM) machine with a dual-stator configuration and high-temperature superconducting materials includes numerous cryogenic components that establish the required operating temperature for superconducting magnets. This abundance of cryogenic elements introduces complexity to the process of conducting a modal analysis of the entire machine. However, the conventional trial-and-error approach employed to achieve precise modal analysis results for the entire-machine suffers from the drawback of lacking a clear direction for adjustment elastic modulus which has a great influence on the modal analysis results. Therefore, it is difficult to obtain accurate modal analysis results of the entire-machine. In response to this challenge, this study focuses on a 10 kW DS-HTS-FM machine as its subject and presents an elastic modulus adjustment method based on the entire-machine modal analysis, aiming to obtain accurate finite element (FE) modal analysis results of the entire-machine. Initially, the FE method is used to find the components that have a great influence on the outer stator modals while the components that have less influence on the outer stator modal are equivalent to the front and rear end cover in the form of additional mass, thus establishing an entire-machine equivalent model for elastic modulus adjustment. Subsequently, an examination is conducted to ascertain the relative impact proportions of the elastic modulus associated with the outer stator, casing, end cover, and armature windings on the natural frequencies of the outer stator, which can lead to a precise determination of the optimal direction for adjusting the elastic modulus parameters. Lastly, based on the entire-machine modal experiment, the elastic modulus of the equivalent model is modified in a definite direction. Consequently, the elastic modulus values for various components of the DS-HTS-FM machine can be accurately identified. Experimental outcomes affirm the efficacy of this approach in attaining precise FE modal results for the DS-HTS-FM machine and reducing the computational time required for FE analysis.

INDEX TERMS Double-stator HTS field-modulated machine, whole-machine equivalent model, elastic modulus, modal experiment.

The associate editor coordinating the review of this manuscript and approving it for publication was Agustin Leobardo Herrera-May.

I. INTRODUCTION

The double stator (DS) high-temperature superconducting (HTS) field modulated (DS-HTS-FM) machine belongs to
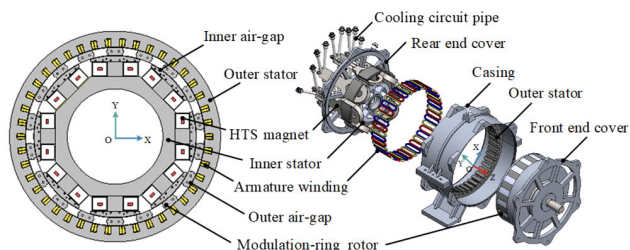
FIGURE 1. 10kW DS-HTS-FM machine structure diagram (a) 2D model (b) Prototype expanded view.
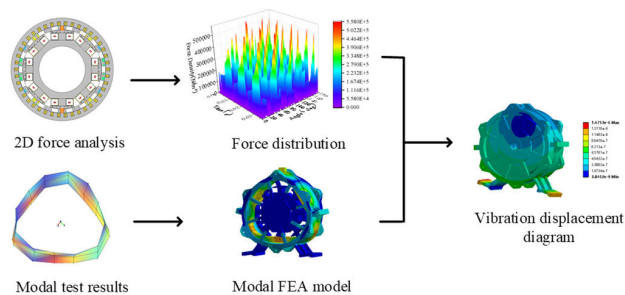

FIGURE 2. Flow chart for the electromagnetic vibration.

the category of stator-excited HTS machines equipped with a stationary seal. Its design principles and operational mechanisms adhere to the principles of magnetic field modulation theory [1], [2]. Fig. 1 presents the 10 kW DS-HTS-FM machine as documented in our earlier investigation [3]. Detailed revelations regarding its mathematical model, cooling computations, and experimental outcomes can be found in [4] and [5]. In terms of strategies employed for cooling and powering the HTS magnets, the DS-HTS-FM machine employs a stationary cooling arrangement and a brushless excitation system. This approach eliminates the need for conventional HTS machines' components such as cryogenic transfer systems, slip rings, and carbon brushes. Therefore, the manufacturing difficulty of the machine is reduced, and the operation reliability of the machine system is improved.

In the DS-HTS-FM machine configuration, HTS magnets are positioned within the inner stator, producing a direct current (DC) excitation field. Subsequently, this excitation field undergoes modulation upon interaction with the rotational rotor, yielding a complex array of harmonic field components within the air gaps—both the inner and outer ones. Situated on the outer stator, the armature windings produce an alternating current (AC) armature field. Similarly, the rotational rotor modulates this armature field, generating a distinct harmonic armature field within the air gaps. The interaction between the harmonic excitation field and the harmonic armature field produces the machine's electromagnetic torque. Additionally, the application of a magnetic field across the air gaps onto the outer stator core gives rise to an electromagnetic force, ultimately leading to radial vibrations and electromagnetic noise [6], [7], [8]. The flow chart of radial vibration of the machine caused by electromagnetic force is illustrated in Fig 2.

Accurately predicting the electromagnetic vibration and noise of the DS-HTS-FM machine necessitates the analysis of electromagnetic force excitation and stator modals [9], [10]. In general, the initial step involves analyzing the radial electromagnetic force exerted on the tooth surface of the stator, followed by accurately determining the stator modal. In these two stages, the radial electromagnetic force can be acquired through both the finite element (FE) method and analytical approaches. The temporal and spatial distribution characteristics of the radial electromagnetic force can be precisely captured by employing the 2D fast Fourier transform [11], [12]. As material properties, including the elastic modulus and Poisson's ratio, undergo changes from raw materials to machine components, the structural modal analysis typically necessitates a combination of FE modeling and modal experimentation. Through fine-tuning material properties in the FE model, it is possible to maintain the modal deviations between experimental and FE model outcomes within an acceptable range [13], [14].

For small-sized machines, modal experiments can be conducted in the unmounted state, allowing for easy adjustment of material properties in the FE model. The unmounted state involves suspending the components using nylon soft ropes [7], [14], [17]. An approach presented in [15] involves correcting the equivalent material parameters of the stator, resulting in a relatively accurate natural frequency prediction with a relative error of less than 3%. Similarly, in [16], material parameters of the stator and windings were determined through modal experiments on stator components. These parameters were then incorporated into the FE model of the entire machine, resulting in modal analysis results with a relative error within 5%. In [17], modal experiments were utilized to identify five anisotropic material parameters. An analytical method for calculating the machine's natural frequency was established based on a theoretical model of the equivalent cylindrical shell. Furthermore, [18], [19] established the characteristic equation for the natural frequency of the stator using an energy method that considers the orthotropic characteristics of laminated core and windings. The accuracy of this proposed method was verified through FE analysis and modal experiments. This study provides valuable insights for the rational adjustment of material parameters.

However, when dealing with large-sized machines, particularly those characterized by low-speed and high-torque operation, performing modal experiments on the stator in the unmounted state presents challenges in terms of safety and feasibility. At this time, the entire-machine modal experiment method with fixed constraints becomes one of the potential solutions. References [20] and [21]. Although this approach offers advantages in terms of ease and safety, it does come with certain drawbacks, such as extended calculation times and increased complexity when adjusting material properties within the FE model. This is primarily due to the larger number of structural components present in the entire machine.

One contributing factor to this challenge is the incomplete quantification of the impact of individual component elastic modulus on the overall machine's modal behavior. As a consequence, the research process often relies on trial-and-error methods for adjustments. In particular, superconducting machines with cryogenic cooling devices have a complex structure and many components compared to conventional large-scale machines, which increases the difficulty of adjusting the elastic modulus of high-temperature superconducting machines.

To address this issue, this study focuses on a 10 kW DS-HTS-FM machine as the subject of investigation. Initially, from a component-level perspective, the FE models are developed for the outer stator, rotor, and inner stator. Subsequently, the effects of elements on the modal behavior of the outer stator are ascertained, leading to the establishment of an equivalent model for the entire machine with adjustable parameters. Furthermore, to clarify the principles governing the adjustment of the elastic modulus in the DS-HTS-FM machine, the influence of the elastic modulus of the outer stator, casing, end covers, and armature windings on the natural frequency of the outer stator is investigated. Finally, the hammer method is employed to acquire modal test results for the entire machine. Based on the equivalent model, the elastic modulus of the outer stator, case, end cover and armature windings are adjusted sequentially so that the error between the simulation results and the experimental results is within 6.6%. This study not only overcomes the difficulty of determining the elastic modulus of the DS-HTS-FM machine, but it also provides a reference for large machines that use the entire-machine modal experiment method to determine elastic modulus parameters, so as to obtain accurate FE results of machine modal analysis. This will be beneficial to the prediction analysis of vibration and noise of the machine.

II. THEORETICAL ANALYSIS OF PARAMETER ADJUSTMENT

Based on the cylindrical shell theory [17], [22], the combined moment of inertia of coaxial cylinders is the sum of the individual moments of inertia of each cylinder. The interrelation of concentrated stiffness among the stator yoke, windings, and casing is posited as parallel. Subsequently, the stator's natural frequency, while taking into account the effects of the stator yoke, windings, and casing, can be expressed as follows [22].

$$f_m \approx \frac{1}{2\pi} \sqrt{\sum_{i=1,2,3} K_{mi}/M_m} \qquad (1)$$

where i=1, 2, 3 represent the stator yoke, windings and casing, respectively. M_m is its total mass, K_{mi} is the corresponding concentrated stiffness.

When the length-to-diameter ratio of the cylindrical shell is less than 1, the analysis and calculation can employ Hoppe's theory. The equations for calculating the equivalent stiffness
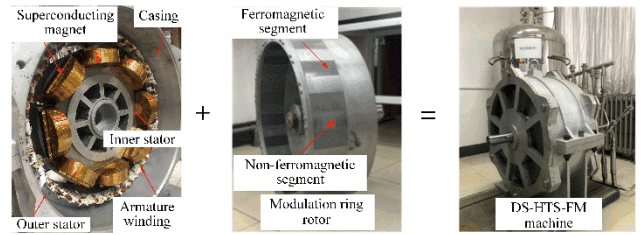

FIGURE 3. DS-HTS-FM machine assembly.

and equivalent mass of the cylindrical shell are given by

$$K_m = \frac{16\pi m^2 (m^2-1)^2}{m^2+1} \frac{EJ}{D^3} \qquad (2)$$

$$M_m = \pi \rho D l h \qquad (3)$$

Here, D, l, and h represent the average diameter, effective length, and wall thickness of the cylindrical shell, respectively. ρ and E denote the equivalent density and elastic modulus of the cylindrical shell. J stands for the moment of inertia of the section parallel to the axis of the cylindrical shell with respect to its axis, and can be expressed as

$$J = \frac{h^3 l}{12} \qquad (4)$$

substituting (2) and (3) into (1) to get

$$f_m = \frac{2}{\pi} \frac{m(m^2-1)}{\sqrt{m^2+1}} \sqrt{\sum_{i=1,2,3} \frac{E_i J_i}{\rho_i l_i h_i D_i^4}} \qquad (5)$$

To assess the impact of the elastic modulus of the stator yoke, windings, and casing on the natural frequency of the stator, the structural parameters such as ρ, l, h, and D are held constant. Under this condition, (5) can be simplified as

$$f_m \propto F_m \sqrt{k_1 E_1 + k_2 E_2 + k_3 E_3} \qquad (6)$$

Here, F_m is the coefficient related to the modal order m. k_1, k_2, and k_3 are the structural parameters of the stator yoke, windings, and casing, respectively. And E_1, E_2, and E_3 are the elastic modulus of the stator yoke, windings, and casing, respectively.

From (6), we can deduce the functional relationship between the stator's natural frequency and the elastic modulus of the stator yoke, windings, and casing. Typically, the elastic modulus is determined based on the material properties of machine components. However, both analytical and FE calculations often rely on idealized material properties, which can introduce significant errors. In the case of FE modeling, it becomes necessary to adjust the elastic modulus for components with anisotropic material properties. Considering the prevalent use of rigid connections in FE modeling, components like the casing and end cover exert a substantial influence on the stator's overall modal behavior in the entire machine model. Hence, it remains essential to adjust the elastic modulus of these components as well. Consequently, conducting a modal analysis on the entire machine becomes

TABLE 1. The key parameters of the prototype.

Parameters	Value	Unit
Outside diameter of outer stator	720	mm
Outside diameter of rotor	610	mm
Inside diameter of rotor	554	mm
Stack length	100	mm
Inner/outer air-gap length	1	mm
Number of outer stator teeth	42	-
Number of inner stator teeth	8	-
Pole-piece number of rotor	18	-
Pole-pair number of armature winding	14	-
Pole-pair number of HTS field winding	4	-
Rated power	10	kW
Rated speed	300	rpm
Rated voltage	380	V
Rated field current of HTS field winding	40	A
Cooling temperature	77	K
Critical curent of HTS coil @ 77 K	70	A

TABLE 2. Initial elastic modulus parameters of DS-HTS-FM machine.

	Young's modulus (MPa)	Shear modulus (MPa)
Outer stator	$E_x=E_y=2.06\times10^5$	$G_{xy}=8.0\times10^4$
	$E_z=1.8\times10^5$	$G_{xz}=G_{yz}=7.2\times10^4$
Armature winding	$E_x=E_y=950$	$G_{xy}=370$
	$E_z=1400$	$G_{xz}=G_{yz}=320$
ZL104	$E=6.9\times10^4$	$G=2.6\times10^4$
Stainless steel	$E=1.9\times10^5$	$G=7.4\times10^5$

imperative in order to establish a set of guidelines for adjusting the elastic modulus of various machine components.

III. ESTABLISHMENT OF EQUIVALENT MODEL OF DS-HTS-FM MACHINE

Fig. 3 illustrates the configuration of the DS-HTS-FM machine. The key parameters of the prototype are listed in Table 1. The machine features an outer stator, which is securely attached to the inner surface of the casing using an interference fit mechanism to accommodate the armature windings. Meanwhile, the inner stator is affixed to the front cover through the inner stator shaft, creating a space for the arrangement of HTS magnets. The rotor assembly consists of a modulation ring rotor, comprising both ferromagnetic and non-ferromagnetic segments. This modulation ring rotor is sandwiched between the inner and outer stators. The two ends of the modulation ring rotor are fastened to the front and rear end covers using bearings for support and stability.

To create a precise equivalent model for the entire machine, it is crucial to analyze how different machine components affect the modal shapes and natural frequencies of the outer stator. As a result, based on the machine's structural layout, the components can be categorized into three sections for equivalent modeling: the outer stator components, the modulation ring rotor components, and the inner stator components.

A. DETERMINATION OF INITIAL MATERIAL PARAMETERS

The natural frequency of the stator is primarily influenced by the elastic modulus and mass density of its constituent components. Mass density can be calculated using the real mass and modeled volume of the machine component. The elastic modulus mainly comprises Young's modulus E and Shear modulus G, whose values are contingent upon the presence of anisotropic material properties in the component. In the case of the outer stator and armature windings, the Z-axis elastic modulus varies from the X and Y-axis directions. This

requires determining four parameters: $E_x = E_y$, E_z, G_{xy}, and $G_{xz} = G_{yz}$. In the context of isotropic materials, where material properties exhibit uniformity in all directions, the determination of only two parameters, E and G, is necessary. Since the outer stator is made of silicon steel sheets laminated along the Z-axis direction, the XOY plane can be regarded as an isotropic material. The value of elastic modulus is set according to the elastic modulus parameter of silicon steel sheet, namely, $E_x = E_y =206$ GPa, $G_{xy} =80$ GPa, and the value of G_{xz} (G_{yz}) is set to 0.9 G_{xy} [20]. However, the value of E_z is determined according to the calculation method of elastic parameters of composite materials [23], namely

$$E_Z = \frac{\varphi_1 E_1(q + E_2) + \varphi_2 E_2(q + E_1)}{\varphi_1(q + E_2) + \varphi_2(q + E_1)} \quad (7)$$

where E_1 is Young's modulus of silicon steel sheet, E_2 is Young's modulus of insulating material, φ_1 and φ_2 are the volume percentage of silicon steel sheet and insulating material, respectively. The q is the empirical fitting constant, whose approximate value can be expressed as

$$q = \frac{\varphi_1 E_1}{2(1 + v_1)} + \frac{\varphi_2 E_2}{2(1 + v_2)} \quad (8)$$

where v_1 and v_2 are the Poisson's ratios of the two materials, respectively.

In (7) and (8), the lamination coefficient of the outer stator is 0.96 and $E_1 =206$ GPa, $E_2 =1.9$ GPa, $v_1 =0.3$, $v_2 =0.35$.

Through the above analysis, the relationship between E_x and E_z, G_{xy}, G_{xz} can be obtained as shown in (9)-(11), where the impact of Poisson's ratio variation on the stator natural frequency can be negligible [24]. So, v_1 and v_2 are set to constant values.

$$G_{xy} = \frac{E_x}{2(1 + v_1)} \approx 0.385E_x \quad (9)$$

$$G_{xz} = G_{yz} = \frac{0.9E_x}{2(1 + v_1)} \approx 0.35E_x \quad (10)$$

$$E_z \approx \frac{\varphi_1 E_x (q + E_2)}{\varphi_1 (q + E_2) + \varphi_2 (q + E_x)}$$
$$\approx \frac{0.36E_x^2 + 1.8E_x}{0.4E_x + 1.8} \approx 0.86E_x \quad (11)$$

The setting of the elastic modulus of armature windings is closely related to whether they are varnished or not. In [20]
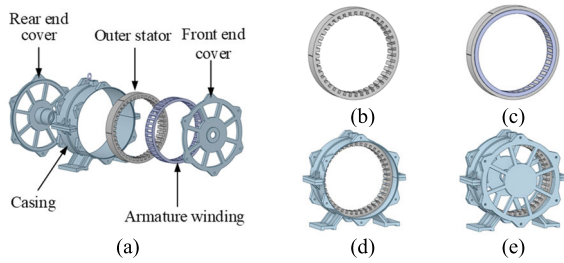
FIGURE 4. Whole outer stator and FE model of modal analysis. (a) Whole outer stator components (b) Model I (c) Model II (d) Model III (e) Model IV.

TABLE 3. Modal analysis results of models I-IV.

FE model	Modal frequency (Hz)			
	2nd	3rd	4th	5th
(I)	111.4	310.2	587	933.5
(II)	92.3	255.4	479.5	756.5
(III)	139.7	443.4	825.6	1159.3
(IV)	470	592.8	878.5	1240.7

and [24], the value of the Young's modulus in the X and Y directions of the varnished windings is 9.5 GPa, which is about 1/10 of the Young's modulus of solid copper, and the value in the Z direction is greater than that of X-axis and Y-axis directions. For the unvarnished winding, the values of Young's modulus in the X-axis and Y-axis directions are significantly smaller than that of the varnished windings, which is about 1/1000 of solid copper [15]. In this paper, the windings of the DS-HTS-FM machine adopts the painting process, so the Young's modulus of the DS-HTS-FM machine armature winding is set to be 1/100 of solid copper [23]. Thus, the elastic modulus of the armature windings is set to $E_x(E_y)$ =950 MPa, E_z =1400MPa, G_{xy} =370 MPa, G_{xz} (G_{yz}) =320 MPa.

The other components of the DS-HTS-FM machine are mainly cast aluminum (ZL104) and stainless steel, which can be regarded as isotropic materials, and the elastic modulus of these components is determined according to their material properties. The initial elastic modulus parameters of the DS-HTS-FM machine are shown in Table 2.

The DS-HTS-FM machine is composed of a large number of individual components. When establishing the FE model of the complete machine as shown in Fig 1 (b), the computational burden and time needed for elastic modulus adjustments become significant. Considering the differing effects of machine components on the outer stator modal, replacing less impactful components with equivalent masses can expedite calculations. Consequently, according to the actual machine configuration, FE models designated as I-VIII are developed. Models I-IV pertain to the entire outer stator, models V-VI relate to the complete modulation ring rotor, and models VII-VIII cover the full inner stator. As a result, modal analysis can be executed for these models.
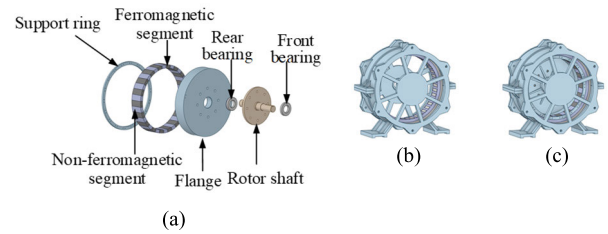

FIGURE 5. Whole rotor and FE model of modal analysis. (a) Whole rotor components (b) Model V (c) Model VI.

TABLE 4. Modal analysis results of Model V and Model VI.

FE model	Modal frequency (Hz)			
	2nd	3rd	4th	5th
(V)	417	530.9	810	1166.8
(VI)	418.2	531.4	811.4	1168.6

B. MODAL ANALYSIS OF WHOLE OUTER STATOR

Fig.4 illustrates the entirety of the outer stator, comprising the outer stator itself, armature windings, casing, and front and rear end covers. Four FE models have been created: FE Model I, representing the outer stator core; FE Model II, encompassing the outer stator and armature windings; FE Model III, combining the outer stator with the casing; and FE Model IV, involving the outer stator, casing, and end covers. Within these FE models, rigid connections exist between the casing and the outer stator, as well as between the casing and the end cover. This leads to close-fitting contact relationships among these components, eliminating relative displacements. The results of the modal analysis are presented in Table 3.

Table 3 reveals a noteworthy observation: the armature windings contribute to a reduction in the natural frequency of the outer stator modes. This implies that the impact of the armature windings on the mass of the outer stator outweighs the influence of the stiffness K, as indicated in (1). In contrast, the casing and end covers exert a more significant effect on the stiffness of the outer stator compared to the mass, leading to an increased natural frequency of the outer stator modes. As a result, it is evident that the armature windings, casing, and front and rear end covers are indispensable components to be incorporated into the equivalent model of the entire machine.

C. MODAL ANALYSIS OF WHOLE MODULATION RING ROTOR

As illustrated in Fig. 5, the complete rotor assembly comprises essential components such as the modulation-ring rotor, support ring, flange, rotor shaft, and bearings. The dynamics of the outer stator modal are influenced by the entirety of the rotor components, transmitted through both the end cover and the casing. To capture this interaction, we have established two FE models: FE Model V, encompassing the outer stator, armature windings, casing, end covers,
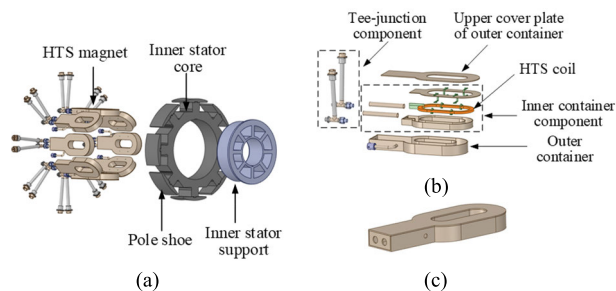
FIGURE 6. Whole inner stator and equivalent magnet (a) Whole inner stator (b) HTS magnet (c) Equivalent magnet.
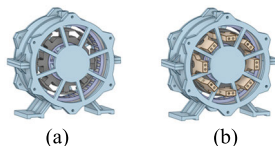

FIGURE 7. FE model of modal analysis of whole inner stator (a) Model VII (b) Model VIII.

TABLE 5. Modal analysis FE results of model VII and Model VIII.

FE model	Modal frequency (Hz)			
	2nd	3rd	4th	5th
(V)	417	530.9	810	1166.8
(VII)	416.7	531.8	811.5	1167.2
(VIII)	417.6	532.4	813.9	1168.1

and their interconnected parts; and FE Model VI, which incorporates the outer stator, armature windings, casing, end covers, and the complete rotor assembly. In both these FE models, we have opted for the rigid connections between the bearings and the shaft, as well as between the bearings and the end covers. With the appropriate initial material parameters in place, the modal analysis outcomes for Model V and Model VI can be computed, as presented in Table 4.

As shown in Table 4, the whole modulation ring rotor has little influence on the 2nd, 3rd, 4th, and 5th natural frequencies of the outer stator, namely it has the same effect on the mass and stiffness of the outer stator. Therefore, it can be considered that the FE model V and the FE model VI are equivalent to each other.

D. MODAL ANALYSIS OF WHOLE INNER STATOR

The entirety of the inner stator comprises essential constituents such as the inner stator support, inner stator core, pole shoes, and HTS magnets. Notably, the HTS magnet is composed of several elements including the outer container component, inner container component, and tee-junction component. Due to the rigid connection between the outer container component and the inner stator, it is feasible to replace the HTS magnet with the outer container component to expedite simulations. Consequently, an equivalent magnet configuration can be derived, as depicted in Fig. 6 (c).

TABLE 6. Modal frequencies of the models V-VIII under the constraint of the bottom angle.

FE model	Modal frequency (Hz)			
	2nd	3rd	4th	5th
(V)	-	517.5	856.7	1117.1
(VI)	412.3	518.1	859.2	1118.2
(VII)	418.5	517.4	860.7	1117.5
(VIII)	-	518.5	865.2	1117.4

As depicted in Fig. 7, two FE models have been established to investigate the impact of the inner stator and the equivalent magnets on the 2nd, 3rd, 4th, and 5th natural frequencies of the outer stator. Specifically, these models are designated as FE Model VII, which includes FE Model V along with the inner stator core, inner stator support, and pole shoes; and FE Model VIII, which encompasses FE Model VII and the equivalent magnets. In both these models, a rigid connection is employed for the inner stator support and the rear end cover. The results of the modal analysis are presented in Table 5.

The information in Table 5 indicates that the deviation in modal frequencies of the same order for FE Models VII, VIII, and V is consistently below 1%. Based on this, it is reasonable to deduce that their impact on the mass and stiffness of the outer stator is quite similar. In other words, the modal frequency of the outer stator appears to be minimally influenced by both the inner stator and the equivalent magnet. Consequently, Models V, VII, and VIII can be regarded as being effectively equivalent to each other.

Based on the information provided earlier, a conclusion can be drawn that the overall rotor and inner stator exert minimal influence on the modal frequencies of the outer stator. Additionally, considering that the end covers play a more significant role in altering the stiffness of the outer stator compared to their effect on mass, it can be inferred that both the complete rotor and the entire inner stator can be treated as equivalent to the front and rear end covers in the form of added mass. Consequently, FE Model V has the potential to be used as a substitute for the entire machine, as depicted in Fig. 1 (b), when carrying out subsequent adjustments to the elastic modulus of the complete machine. This simplification would aid in the process of fine-tuning the modal characteristics of the complete system.

IV. ANALYSIS OF ADJUSTMENT RULES OF ELASTIC MODULUS

Based on the above analysis, the influence of the elastic modulus of the machine components on the natural frequency of the outer stator is complex, and the direction of elastic modulus adjustment is not clear. It is necessary to quantitatively analyze the influence of these components on the 2nd, 3rd, 4th, and 5th natural frequencies of the outer stator so that the adjustment rules of the elastic modulus of these components can be clarified.
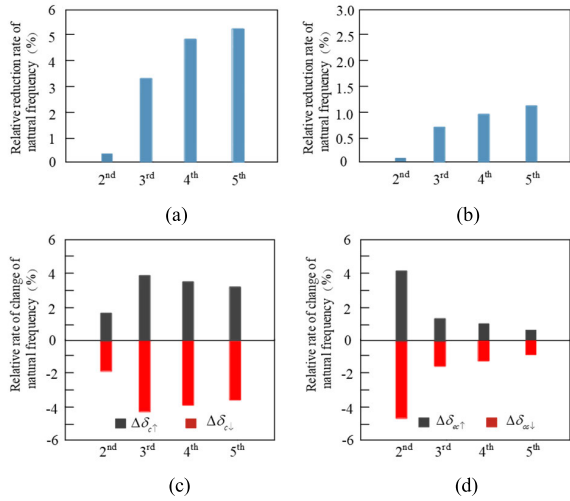
FIGURE 8. Relative change rate of 2nd, 3rd, 4th and 5th natural frequencies of outer stator. (a) Eos=0.75Eos0. (b) Eaw=0.75Eaw0 (c) Ec=0.85Ec0 and Ec=1.15Ec0, (d) Eec=0.85Eec0 and Eec=1.15Eec0.

FIGURE 9. The flow chart of the elastic modulus adjustment of the entire machine.

A. SELECTION OF DS-HTS-FM MACHINE FE MODEL UNDER THE CONSTRAINT OF THE BOTTOM ANGLE

In the context of the DS-HTS-FM machine, conducting free modal tests might pose challenges. As an alternative approach, this research delves into investigating the equivalent model of the entire machine while considering the constraint of the bottom angle. The objective is to reveal the proportional influence of the elastic modulus of different machine components on the natural frequencies. Following the analytical procedure detailed in Section III, the modal analysis results for models V to VIII, all under the constraint of the bottom angle, are presented in Table 6. These results offer insights into how varying the elastic modulus of different components impacts the modal characteristics within the given constraint framework.

It can be seen from Table 6 that the modal analysis results of models V-VIII have little difference after applying bottom angle constraints. So these models can still be considered to be equivalent to each other. It should be noted that the 2nd modal shape of the FE model V is not obvious, so this model is not suitable as an equivalent model for the whole-machine. Besides, considering that the FE model VII contains fewer components than those of model VI, the FE model VII is selected as the whole machine equivalent model to reduce the calculation time.

B. ELASTIC MODULUS ADJUSTMENT RULE OF DS-HTS-FM MACHINE

Firstly, the material parameters determined in Table 2 are taken as the initial values for parameter adjustment of machine components. The elastic modulus values of the outer stator, armature windings, casing, and end covers are adjusted on the basis of these initial values. And then, to clarify the adjustment direction of elastic modulus in FE model VII, the relative change rate of the outer stator natural frequency was calculated according to (12)-(15). Due to lamination effects,
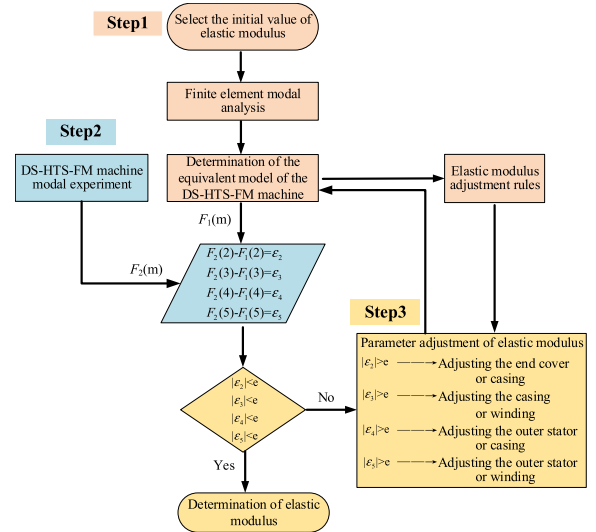
the elastic modulus of the outer stator and windings are lower than those of solid steel and copper, so the elastic modulus value of the outer stator and windings is smaller than the initial value.

$$\Delta\delta_{os\downarrow} = \frac{f(E_{os0}) - f(E_{os\downarrow})}{f(E_{os0})} \times 100\% \tag{12}$$

$$\Delta\delta_{aw\downarrow} = \frac{f(E_{aw0}) - f(E_{aw\downarrow})}{f(E_{aw0})} \times 100\% \tag{13}$$

$$\Delta\delta_{c\uparrow(\downarrow)} = \frac{f(E_{c\uparrow(\downarrow)}) - f(E_{c0})}{f(E_{c0})} \times 100\% \tag{14}$$

$$\Delta\delta_{ec\uparrow(\downarrow)} = \frac{f(E_{ec\uparrow(\downarrow)}) - f(E_{ec0})}{f(E_{ec0})} \times 100\% \tag{15}$$

where f is the natural frequency of the outer stator, $\Delta\delta_{os\downarrow}$, $\Delta\delta_{aw\downarrow}$, $\Delta\delta_{c\uparrow(\downarrow)}$, $\Delta\delta_{ec\uparrow(\downarrow)}$ is the change rate of the natural frequency of the machine when the elastic modulus of the outer stator, armature winding, casing and end covers are adjusted, respectively, E_{os0}, E_{aw0}, E_{c0}, E_{ec0} are the elastic modulus initial values of the outer stator, armature winding, casing and end covers respectively, $E_{os\downarrow}$ and $E_{aw\downarrow}$ are the adjustment values of the outer stator and armature windings when the elastic modulus has already been adjusted downwards, while $E_{c\uparrow(\downarrow)}$ and $E_{ec\uparrow(\downarrow)}$ are the adjustment values of the casing and end covers when the elastic modulus has already been adjusted upwards or downwards, respectively.

Finally, the relative change rate of the 2nd, 3rd, 4th, and 5th natural frequencies of the machine are depicted as shown in Fig. 8 when the elastic modulus of the outer stator, armature windings, casing, and end covers have been adjusted. Among them, Fig. 8(a), the E_{os} =0.75 E_{os0}; Fig. 8(b), the E_{aw} =0.75E_{aw0}; Fig. 8(c), the E_c =0.85 $E_{c0}$and E_c =1.15 E_{c0}; Fig. 8(d), the E_{ec} =0.85 E_{ec0} and E_{ec} =1.15 E_{ec0}.

In Fig. 8(c) and Fig. 8(d), when the elastic modulus is adjusted downward or upward by the same value, $|\Delta\delta_\downarrow|$ is greater than $|\Delta\delta_\uparrow|$. In addition, the adjustment of the outer
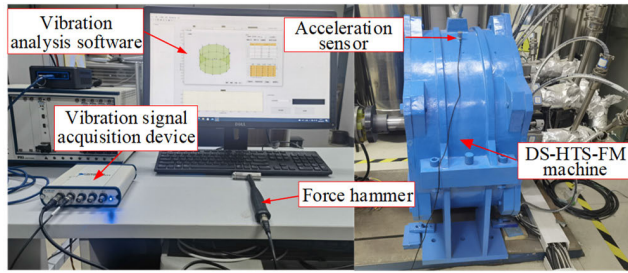
FIGURE 10. Modal test platform of DS-HTS-FM machine.

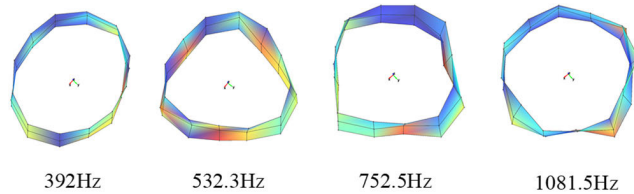| 392Hz | 532.3Hz | 752.5Hz | 1081.5Hz |

FIGURE 11. Mode shapes and natural frequencies obtained from modal experiments.

stator elastic modulus has a small influence on the 2nd natural frequency, but a significant influence on the 3rd, 4th, and 5th. The adjustment of armature windings elastic modulus has a relatively small influence on each order natural frequency and can be used for fine-adjustment of the 3rd, 4th, and 5th order natural frequencies. The adjustment of the casing elastic modulus on the 2nd order is relatively small, however, the adjustment of the end cover has a relatively large influence on the 2nd order. Also, the influence degree on the 3rd, 4th, and 5th order natural frequencies of both casing and end cover decreases in turn.

C. ELASTIC MODULUS ADJUSTMENT METHOD OF THE WHOLE-MACHINE

Fig. 9 is the flow chart of the elastic modulus adjustment of the entire-machine. Step 1 involves setting the initial value of the elastic modulus based on the actual structure of the DS-HTS-FM machine. After this initial setup, a FE modal analysis is conducted on the machine model. This analysis results in the establishment of an equivalent model for parameter adjustment. In addition, the FE results of the modal analysis $F_1(m)$ and the elastic modulus adjustment rule are obtained. In step 2, a whole machine modal test platform is built to obtain the modal test results $F_2(m)$. Then the relative errors ε_2, ε_3, ε_4, and ε_5 of the 2nd, 3rd, 4th, and 5th order modal frequencies are obtained by comparing $F_1(m)$ with $F_2(m)$, respectively. In step 3, according to the adjustment rules for the elastic modulus, $F_1(m)$ is adjusted as closely as possible to $F_2(m)$ until the error meets the requirements.

V. PARAMETER ADJUSTMENT OF ELASTIC MODULUS

Before the adjustment of elastic modulus, it is necessary to use a whole-machine modal experiment to obtain the modal frequency and modal shape, which will be used as the basis for adjusting the elastic modulus of the FE model. Then, considering the errors of the experiment and FE analysis results,

TABLE 7. Comparison of whole-machine modal experiment and FE results based on the initial value.

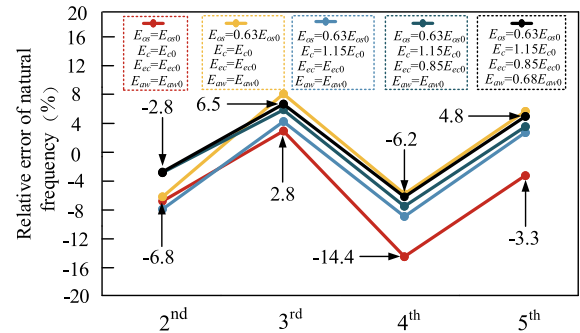| Order	FE result (Hz)	Test result (Hz)	Error (%)
2nd	418.5	392	-6.8
3rd	517.4	532.3	2.8
4th	860.7	752.5	-14.4
5th	1117.5	1081.5	-3.3

FIGURE 12. Error variations under elastic modulus adjustment.

TABLE 8. Elastic modulus parameters of the whole-machine model.

Machine component	Young's modulus (MPa)	Shear modulus (MPa)
Outer stator	$E_x=E_y=1.3\times10^5$	$G_{xy}=5\times10^4$
	$E_z=1.1\times10^5$	$G_{xz}=G_{yz}=5\times10^4$
Armature winding	$E_x=E_y=650$	$G_{xy}=250$
	$E_z=1000$	$G_{xz}=G_{yz}=230$
Casing	$E=7.9\times10^4$	$G=2.95\times10^4$
End cover	$E=5.9\times10^4$	$G=2.2\times10^4$

and adjusting the elastic module value based on the adjustment rules, a more accurate FE model of the whole-machine can be obtained
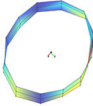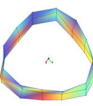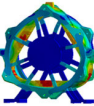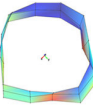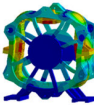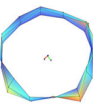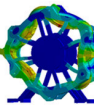
A. MODAL EXPERIMENT OF THE WHOLE-MACHINE

The DS-HTS-FM machine modal test platform is shown in Fig.10. Due to the large volume of the whole-machine, the constraint of the bottom angle has been adopted instead of its free state. And to reduce the effect of ground stiffness on the motor, the base is cushioned with rubber pads underneath. In this paper, the force hammer is used as the exciting device to excite the modals of the DS-HTS-FM machine to produce vibration signals. The response signals are transmitted to the data acquisition and vibration signal analyzer by the acceleration sensor. The vibration analysis software calculates the input and output signals processed by the vibration signal analyzer. Then, by processing the frequency response functions at each measurement point, the 2nd, 3rd, 4th, and 5th order mode shapes and natural frequencies of the DS-HTS-FM machine are obtained, as shown in Fig. 11.

B. DETERMINATION OF ELASTIC MODULUS PARAMETERS

The elastic modulus initial values listed in Table 2 are brought into the whole-machine equivalent model VII to get the FE

TABLE 9. Comparison of whole-machine modal experiment and FE results.

Order	Test result	FE result	Error
2nd	392Hz	402.4Hz	-2.6%
3rd	532.3Hz	501.5Hz	5.8%
4th	752.5Hz	802.1Hz	-6.6%
5th	1081.5Hz	1031.1Hz	4.7%

modal analysis results. The comparisons between the FE modal analysis and the experimental results are shown in Table 7. It can be seen that the 4th order error of modal frequency is large, and the 2nd, 3rd, and 5th order errors of modal frequency are small.

In order to adjust modal frequency order errors as small as possible, the elastic modulus of outer stator, casing, end cover and armature windings are successively set to 0.63 Eos0, 0.85 Ec0, 0.85 Eec0, 0.68 Eaw0 based on the elastic modulus adjustment rules shown in Fig.8, respectively. Then the variation of natural frequency error of each order can be calculated as shown in Fig. 12. It can be seen that the 2nd, 3rd, 4th, and 5th errors of the outer stator are all within 6.5% after adjusting the elastic modulus of machine components. Accordingly, the elastic modulus values of machine components in the whole-machine equivalent model can be determined as shown in Table 8.

In order to further verify the accuracy of the above analysis, the whole-machine model shown in Fig.1 (b) was used calculate the error between the FE results and test results. In Fig.1 (b), the whole inner stator and the whole modulation-ring rotor applied the initial value of elastic modulus according to Table 2, and the whole outer stator applied the adjustment value of elastic modulus based on Table 8. The modal shape and natural frequency comparison are shown in Table 9. To better show the modal shapes of the whole-machine, other components except for the outer stator, casing, end cover, and armature windings have been hidden.

The results in Table 9 show that the natural frequency errors of each order for the whole-machine are within 6.6%, providing evidence of obtaining more accurate FE modal results. Therefore, this analysis method overcomes the limitation of adjusting the whole-machine's elastic modulus, benefiting the prediction and analysis of vibration and noise.

VI. CONCLUSION

In this paper, a method for adjusting the elastic modulus is proposed by using entire machine modal analysis, which aims to overcome the problem that it is difficult to accurately determine the modal analysis FE results of high-temperature superconducting machines and large machines. The study focuses on a 10 kW DS-HTS-FM machine, conducting modal analyses for the entire outer stator, rotor, and inner stator through eight sets of FE models. The outcome is the identification of an equivalent model representing the combined outer stator and inner stator core, serving as the basis for entire-machine elastic modulus adjustments. By manipulating the elastic modulus of various components such as the outer stator, casing, end cover, and armature windings, the research quantifies the relative impact of these elements on the 2nd, 3rd, 4th, and 5th natural frequencies of the outer stator. This allows for a clearer understanding of the directional adjustments needed for the elastic modulus. Subsequently, based on the entire-machine modal experiment, adjustments are made to each order of natural frequencies of the DS-HTS-FM machine to ensure they fall within a 6.6% error range. The results show that this method can clarify the adjustment direction of the elastic modulus for the entire machine model, and then obtain accurate FE modal analysis results for the entire machine, which will be beneficial for the subsequent vibration and noise prediction analysis of the machine.

REFERENCES

[1] M. Cheng, P. Han, and W. Hua, "General airgap field modulation theory for electrical machines," *IEEE Trans. Ind. Electron.*, vol. 64, no. 8, pp. 6063–6074, Aug. 2017.

[2] S. Wang, K. Lin, M. Lin, Y. Kong, D. Xu, N. Li, and P. Wang, "Comparative study of E- and U-core modular dual-stator axial-field flux-switching permanent magnet motors with different stator/rotor-pole combinations based on flux modulation principle," *IEEE Access*, vol. 9, pp. 78635–78647, 2021.

[3] M. Cheng, X. Zhu, Y. Wang, R. Wang, and W. Wang, "Effect and inhibition method of armature-reaction field on superconducting coil in field-modulation superconducting electrical machine," *IEEE Trans. Energy Convers.*, vol. 35, no. 1, pp. 279–291, Mar. 2020.

[4] Y. Wang, Q. Wang, X. Zhu, X. Li, and W. Hua, "An improved critical current calculation method of HTS field-excitation coil for double-stator HTS generator with stationary seal," *IEEE Trans. Energy Convers.*, vol. 38, no. 1, pp. 624–635, Mar. 2023.

[5] X. Zhu, M. Cheng, X. Li, and Y. Wang, "Topology analysis, design, and comparison of high temperature superconducting double stator machine with stationary seal," *IEEE Trans. Appl. Supercond.*, vol. 30, no. 1, pp. 1–10, Jan. 2020.

[6] Y. Wang, W. Xu, X. Zhang, and W. Ma, "Harmonic analysis of air gap magnetic field in flux-modulation double-stator electrical-excitation synchronous machine," *IEEE Trans. Ind. Electron.*, vol. 67, no. 7, pp. 5302–5312, Jul. 2020.

[7] Y. Wang, C. Zhao, and X. Li, "Vibration and noise analysis of flux-modulation double stator electrical-excitation synchronous machine," *IEEE Trans. Energy Convers.*, vol. 36, no. 4, pp. 3395–3404, Dec. 2021.

[8] H. Wang and S. Ding, "Design and analysis of new dual-stator field modulation machines with multiple magnetic excitations," *IEEE Trans. Magn.*, vol. 57, no. 2, pp. 1–6, Feb. 2021.

[9] D. Torregrossa, F. Peyraut, B. Fahimi, J. M'Boua, and A. Miraoui, "Multiphysics finite-element modeling for vibration and acoustic analysis of permanent magnet synchronous machine," *IEEE Trans. Energy Convers.*, vol. 26, no. 2, pp. 490–500, Jun. 2011.

[10] S. Cho, J. Hwang, and C.-W. Kim, "A study on vibration characteristics of brushless DC motor by electromagnetic-structural coupled analysis using entire finite element model," *IEEE Trans. Energy Convers.*, vol. 33, no. 4, pp. 1712–1718, Dec. 2018.

[11] S. Taghipour Boroujeni and V. Zamani, "A novel analytical model for no-load, slotted, surface-mounted PM machines: Air gap flux density and cogging torque," *IEEE Trans. Magn.*, vol. 51, no. 4, pp. 1–8, Apr. 2015.

[12] F. Lin, S. Zuo, and X. Wu, "Electromagnetic vibration and noise analysis of permanent magnet synchronous motor with different slot-pole combinations," *IET Electr. Power Appl.*, vol. 10, no. 9, pp. 900–908, 2016.

[13] F. Lin, S. Zuo, W. Deng, and S. Wu, "Noise prediction and sound quality analysis of variable-speed permanent magnet synchronous motor," *IEEE Trans. Energy Convers.*, vol. 32, no. 2, pp. 698–706, Jun. 2017.

[14] Y. Fang and T. Zhang, "Vibroacoustic characterization of a permanent magnet synchronous motor powertrain for electric vehicles," *IEEE Trans. Energy Convers.*, vol. 33, no. 1, pp. 272–280, Mar. 2018.

[15] H. Yin, F. Ma, X. Zhang, C. Gu, H. Gao, and Y. Wang, "Research on equivalent material properties and modal analysis method of stator system of permanent magnet motor with concentrated winding," *IEEE Access*, vol. 7, pp. 64592–64602, 2019.

[16] S. Hu, S. Zuo, M. Liu, and H. Wu, "Method for acquisition of equivalent material parameters considering orthotropy of stator core and windings in SRM," *IET Electr. Power Appl.*, vol. 13, no. 4, pp. 580–586, Apr. 2019.

[17] S. Hu, S. Zuo, H. Wu, and M. Liu, "An analytical method for calculating the natural frequencies of a motor considering orthotropic material parameters," *IEEE Trans. Ind. Electron.*, vol. 66, no. 10, pp. 7520–7528, Oct. 2019.

[18] Z. Xing, X. Wang, and W. Zhao, "An accurate calculation method of natural frequencies of the radial-flux slotted motors considering end covers," *IEEE Trans. Ind. Electron.*, vol. 70, no. 6, pp. 5516–5526, Jun. 2023.

[19] Z. Xing, X. Wang, W. Zhao, L. Sun, and N. Niu, "Calculation method for natural frequencies of stator of permanent magnet synchronous motors based on three-dimensional elastic theory," *IEEE Trans. Energy Convers.*, vol. 36, no. 2, pp. 755–766, Jun. 2021.

[20] T. Y. Wang and F. X. Wang, "Vibration and modal analysis of stator of large induction motors," *Proc. Chin. Soc. Elect. Eng.*, vol. 27, no. 12, pp. 41–45, Nov. 2007.

[21] Z. Liu, Y. Xiang, and Y. Zhou, "Finite element modeling method and modal analysis of a high temperature superconducting motor," *IEEE Trans. Appl. Supercond.*, vol. 31, no. 8, pp. 1–4, Nov. 2021.

[22] S. M. Castano, B. Bilgin, E. Fairall, and A. Emadi, "Acoustic noise analysis of a high-speed high-power switched reluctance machine: Frame effects," *IEEE Trans. Energy Convers.*, vol. 31, no. 1, pp. 69–77, Mar. 2016.

[23] F. Chai, Y. Li, Y. Pei, and Z. Li, "Accurate modelling and modal analysis of stator system in permanent magnet synchronous motor with concentrated winding for vibration prediction," *IET Electr. Power Appl.*, vol. 12, no. 8, pp. 1225–1232, Sep. 2018.

[24] W. Deng, Z. Qian, W. Chen, C. Qian, and Q. Wang, "Orthotropic material parameters identification method of stator core and windings in electric motors," *IEEE Trans. Energy Convers.*, vol. 38, no. 4, pp. 2464–2474, Dec. 2023.

CHUNTONG SONG was born in Shandong, China, in 1997. He received the B.S. degree in electrical engineering and automation from the College of Electrical Engineering and Automation, Qilu University of Technology, Jinan, China, in 2021. He is currently pursuing the M.Sc. degree in electrical engineering with the China University of Petroleum (East China).

His research interest includes vibration and noise analysis of high temperature superconducting generators.

ZHIHENG ZHANG (Graduate Student Member, IEEE) was born in Luoyang, Henan, China, in 1994. He received the B.S. degree from the College of Electrical Engineering and Automation, Zhengzhou University of Light Industry, Zhengzhou, China, in 2017, and the M.S. degree in electrical engineering from the School of Electrical Engineering, Shenyang University of Technology, Shenyang, China, in 2020. He is currently pursuing the Ph.D. degree in electrical engineering with the School of Electrical Engineering, Southeast University, Nanjing, China.

His research interests include the design, analysis, and control of electrical machines and industrial machinery.

YUBIN WANG was born in Shandong, China. He received the M.Sc. degree in control theory and control engineering from the College of Electrical Engineering and Automation, Shandong University of Science and Technology, Jinan, China, in 2003, and the Ph.D. degree in electrical engineering from the Department of Electrical Engineering, Southeast University, Nanjing, China, in 2011.

Since 2003, he has been with the China University of Petroleum (East China), where he is currently a Professor with the College of New Energy. From September to December 2013, he was a Research Assistant with the Department of Electrical and Electronic Engineering, The University of Hong Kong. He is the author or coauthor of more than 30 technical articles, and he is the holder of ten patents in his areas of interest. His research interests include electromagnetic design and analysis of high temperature superconducting generators with stationary seal and permanent magnet machines.

WEI HUA (Senior Member, IEEE) received the B.Sc. and Ph.D. degrees in electrical engineering from Southeast University, Nanjing, China, in 2001 and 2007, respectively.

From 2004 to 2005, he was with the Department of Electronics and Electrical Engineering, The University of Sheffield, U.K., as a Joint-Supervised Ph.D. Student. Since 2007, he has been with Southeast University, where he is currently a Chief Professor and a Distinguished Professor of Jiangsu Province. Since 2010, he has been with the Yancheng Institute of New Energy Vehicles, Southeast University. He has coauthored more than 150 technical articles. He holds 50 patents in his areas of interest. His research interests include design, analysis, and control of electrical machines, especially for PM brushless machines and switching reluctance machines.

● ● ●